Confined Concrete-Filled Tubular Columns

Yan Xiao[1]; Wenhui He[2]; and Kang-kyu Choi[3]

Abstract: This paper presents a study to introduce and experimentally validate an innovative concrete filled steel tubular (CFT) column system, named as confined CFT or CCFT, for improved seismic design of steel and concrete composite structures. Based on fundamental mechanics, the concept is aimed at controlling the local buckling of the steel tube and confining the concrete in the potential plastic hinge regions of a CFT column. To achieve this, several efficient details of transverse confinement are proposed. In the first phase of the study, carbon-fiber-reinforced plastic as additional confinement of CCFT columns was examined through experimental testing. As demonstrated from the results of axial compression tests and seismic loading tests, the new type of CFT column system can provide excellent seismic performance. The complicated local buckling and confinement mechanisms were examined using a proposed simple analytical model.

DOI: 10.1061/(ASCE)0733-9445(2005)131:3(488)

CE Database subject headings: Columns; Buckling; Seismic response; Ductility; Confinement.

Introduction

Background

The proposed new concrete filled tubular (CFT) column is conceived by the first writer based on previous research on two steel tubular column structural systems: the CFT column and the tubed column. The two different but related systems are shown in Fig. 1 and are briefly described below.

CFT Column

In a conventional CFT column system, concrete is filled in steel tubes, which typically continue throughout several stories or the full-height of a building (e.g., Moor and Gosain 1985; Viest et al. 1997). The steel tube is expected to carry stresses primarily in the longitudinal direction caused by axial loading and moments, as well as in the transverse direction caused by shear and the internal passive pressure due to concrete dialation, i.e., the confining stress.

Tubed Column

The concept of using a steel tube as primarily transverse reinforcement for reinforced concrete (RC) columns was first studied by a research group lead by Tomii (Tomii et al. 1985a,b; Xiao et al. 1986a,b; Tomii et al. 1987). The terminology of "tubed column" first adopted by Tomii et al. (1985a,b) refers to the function of the tube as that of the hoops in a hooped RC column. Thus the composite action between the steel tube and concrete is primarily expected in the transverse direction only for a tubed column.

Conventional CFT Columns

In recent years, CFT structures have become more widely accepted and used in tall buildings as well as arch bridges, particularly in the far-east region, like China and Japan. The advantages of conventional CFT column structures include:

1. As a typical composite structural system, due to the composite effects, the advantages of two materials can be utilized and their disadvantages can be compensated, thus forming a more rational system.
2. Compared with steel structures, the cost can be reduced by using composite or hybrid systems, since the reduced usage of steel would result in increased stiffness as well as improved fire resistance.
3. The steel tubes can be used as the formwork and the shoring system for casting concrete in construction, thus CFT structures have improved constructability than typical reinforced concrete structures.

However, the conventional CFT system also has its own disadvantages, such as

1. The beam-to-column connections are complicated for CFT frame structures. In Japan, structural frames using CFT columns typically adopt steel or SRC beams with specially designed connections, thus increasing the construction cost. Practices in China tend to use more CFT-column and RC-beam systems with complicated connections (examples can be found in Xiao and Mahin 2000).
2. Due to the fact that a steel tube is used as longitudinal reinforcement to resist axial force and moment, when steel tube yields under excessive longitudinal stresses due to moment or axial load, its transverse confinement (particularly in terms of stiffness) to the internal concrete is drastically reduced. This may be considered as the fate of steel as an isotropic material.
3. As demonstrated in the cyclic loading tests of conventional CFT columns conducted by Sakino (Sakino and Tomii 1981; Council 1992), local plastic buckling may occur at the ends of the steel tube followed by the crushing of internal con-

[1]Associate Professor, Dept. of Civil and Environmental Engineering, Univ. of Southern California, Los Angles, CA 90089; Cheung Kong Scholar, Hunan Univ. E-mail: yanxiao@usc.edu

[2]Research Assistant, Hunan Univ., China.

[3]Graduate Research Assistant, Dept. of Civil and Environmental Engineering, Univ. of Southern California, Los Angles, CA 90089.

Note. Associate Editor: Sashi K. Kunnath. Discussion open until August 1, 2005. Separate discussions must be submitted for individual papers. To extend the closing date by one month, a written request must be filed with the ASCE Managing Editor. The manuscript for this paper was submitted for review and possible publication on November 26, 2003; approved on May 21, 2004. This paper is part of the ***Journal of Structural Engineering***, Vol. 131, No. 3, March 1, 2005. ©ASCE, ISSN 0733-9445/2005/3-488–497/$25.00.

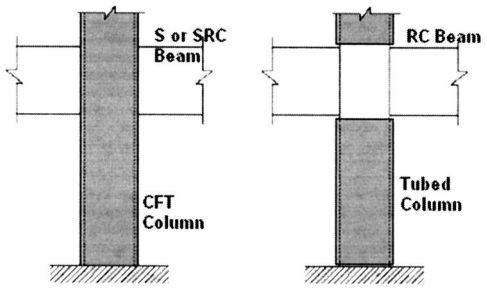

Fig. 1. Two different tubular column systems: (a) CFT column and (b) tubed column

crete. This type of failure is very difficult to repair if not impossible. Such failure mode also results in unstable hysteretic loading capacity, particularly for columns with higher axial load.

Development of Tubed RC Column

The tubed column system was developed to improve some of the disadvantages of the conventional CFT columns. A brief review is summarized below, from a more comprehensive discussion by Xiao (2001).

In Tomii et al.'s original studies (1985a,b; 1987), the tubed RC column concept was investigated as a method to prevent shear failure and to improve the ductility of short columns in RC frame structures or boundary columns of shear walls. The steel tubes are used to transversely confine concrete, whereas the ordinary longitudinal reinforcing bars are still needed for providing flexural strength of the columns. The tubed RC column structure can still be considered as a RC structural system, thus connection detailing and other design as well as construction methods used in conventional RC structures are applicable without significant modification.

One of the key features of a tubed RC column is to properly detail the tube to avoid or reduce direct transfer of the longitudinal stresses into the tube, which is designed primarily as transverse reinforcement. This is achieved by providing a gap between the tube and the beam or footing at the ends of a column, as shown in Fig. 1(b). The concept of the tubed column was validated through testing model columns under constant axial load and cyclic shear in double-curvature condition (Tomii et al. 1985a,b; Xiao et al. 1986a,b; Tomii et al. 1987).

Jacketing retrofit of existing deficient RC columns can also be considered as the application of the tubed column concept. For most cases, the jacket is used to provide additional transverse reinforcement to increase the capacity and to improve the ductility of an existing column. This is achieved by welding steel plate shells to enclose an existing column to form a tubed system, same as that shown in Fig. 1(b). Systematic studies on steel jacketing were carried out by Priestley et al. from the late 1980s (Chai et al. 1991; Priestley et al. 1994a,b). For circular columns, welded steel cylindrical shells are used, whereas for rectangular columns, an elliptical jacket is preferred to provide a continuous confinement. However, retrofitting rectangular columns using elliptical jacketing is typically not acceptable for building columns, for the reasons of architectural appearance and functional requirements. Two recent developments may have provided improved solutions of retrofitting rectangular or square columns using rectilinear jackets. Aboutaha et al. (1996) developed and tested a system which combined drilled cross-bolts with rectangular jackets, showing enhanced confinement efficiency. Xiao and Wu (2003) developed a jacketing method to retrofit square columns using welded rectilinear steel jackets and stiffeners.

Significant research efforts have been recently carried out to explore fiber-reinforced-polymer (FRP) composites for retrofitting or strengthening RC structures (ACI 440R 1996; Teng et al. 2000; Xiao 2001). An FRP jacketed column can be categorized as the tubed system, from the fact that the FRP jacket, once installed, forms a tube to provide primarily additional transverse reinforcement to the original column.

Proposed CCFT Column

A new CFT column system is conceived by the first writer following extensive previous research studies on CFT columns and steel or FRP tubed columns. In the new CFT column, additional transverse reinforcement is designed for the potential plastic

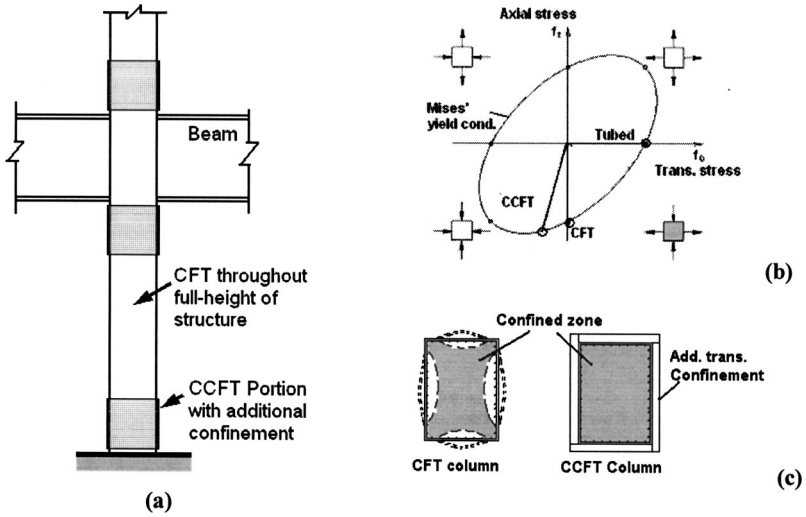

Fig. 2. Proposed CCFT column system: (a) elevation view of a frame portion; (b) different transverse confinement effects in CFT and CCFT; and (c) stress states in different tubes

hinge regions, as illustrated in Fig. 2(a), to achieve improved seismic performance. Based on fundamental mechanics, the design concept is aimed at controlling the local buckling of the steel tube and more efficiently confining concrete in the critical regions of a CFT column. For this reason, the proposed new CFT column system can be named as confined CFT column system, and is referred to as CCFT hereafter.

The CCFT column is expected to overcome disadvantages of the conventional CFT column and to provide the ideal choice for structural design of tall buildings or bridges, particularly for seismic regions. The following are several expected merits of the CCFT column system as compared with the conventional CFT structures.

1. In a CCFT column, the functions of the through-tube (similar to the tube in a conventional CFT column) and the additional transverse reinforcement are separated, the former mainly resists longitudinal stresses caused by axial load and moment as well as shear in the middle portion of the column, whereas the additional reinforcement mainly enhances the potential plastic hinge regions.
2. The additional transverse reinforcement can effectively prevent or delay the local buckling of the through-tube in the plastic hinge regions of a CFT column, thus improving its seismic performance with stable load carrying capacity and ductility.
3. The concrete in the column plastic hinge regions can be more efficiently confined by the additional transverse reinforcement, and as a consequence, the ductility of the column can be assured.
4. Due to the additional transverse confinement, the through-tube in the compression zone of the plastic hinge region is subjected to biaxial compressive stresses (strictly speaking, should be triaxial compression), shown as the third quadrant in Fig. 2(b). This is a more efficient working state for a steel tube as compared with the combination of axial compression and transverse tension, shown in the fourth quadrant in Fig. 2(b), which is the working stress state of the tube in compression zones of a conventional CFT column.
5. In a conventional CFT column, in order to prevent the local buckling of the steel tube in the plastic hinge regions, a relatively thicker steel tube is required, and typically such thickness is provided throughout the length of the column, particularly for columns with a rectangular section. On the other hand, in a CCFT column, the through-tube is designed mainly as longitudinal reinforcement to resist axial load and moment, and is enhanced transversely by the additional transverse reinforcement in the potential plastic hinge regions. The secondary function of the through-tube is to resist shear in the middle portion of the column, and this can typically be achieved by using the same thickness of the through-tube. Efficient details and the confining effects from the joining beams also relaxed the need for a thick steel tube through the connection region. Thus it is expected that even with the addition of the transverse reinforcement for the potential hinge regions, the total amount of steel usage in a CCFT column may be less than the identical CFT column.
6. Apparently, since the additional transverse reinforcement is only provided for the potential plastic hinge regions of the columns, a structural system using CCFT columns remains essentially the same as a CFT structure. Thus design details such as connections developed for conventional CFT structures are still applicable to the proposed CCFT system.

For the design of the additional transverse reinforcement, the following are considered and being evaluated as potential options and are examined in the research program:

1. Additional steel plates or tubes are welded to the potential plastic hinge regions of the through-tube, schematically shown in Fig. 2;
2. Angles, small tubes or pipes, etc., which have larger transverse stiffness and resistance can be used, similar as those proved to be effective to enhance the retrofitting efficiency of rectangular jacketing by Xiao and Wu (2003), as shown in Fig. 2(c).
3. Fiber-reinforced plastics (FRP) can be used to create a new composite system, as shown in this paper; and
4. Reinforced concrete jacketing can be considered, which may also serve as the fire-proof for the steel tube.

A joint research program designed to develop the design methodology of structures with CCFT columns is currently being conducted at the University of Southern California and the Hunan University. This paper describes the concept of CCFT and the results of the experimental validation to support the idea. In the current study, both welded steel and carbon-fiber-reinforced plastics (CFRP) are used as additional confinement for CCFT columns (Xiao et al. 2003), however, this paper focuses on the discussion of experimental results of CCFT columns with CFRP confinement.

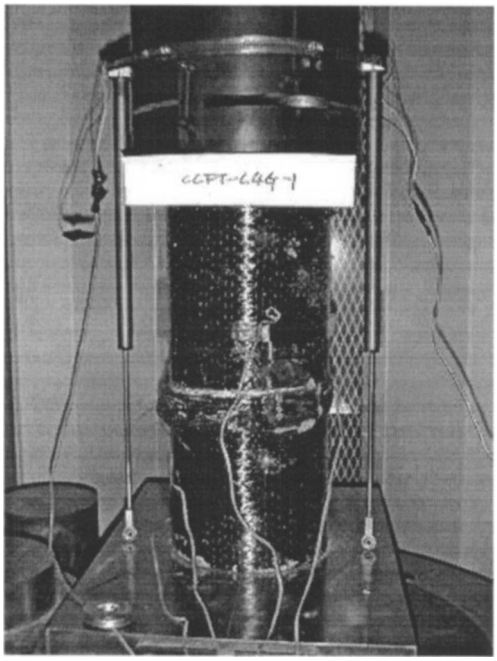

Fig. 3. Axial compression test setup

Mechanical Behavior of CCFT under Compression

Compression Test Specimens

In order to validate the basic mechanical concepts of CCFT columns, 13 cylinder specimens were tested under monotonic axial compression using the 500 t capacity high-stiffness compression testing machine at the USC Structural Laboratory, shown in Fig. 3. In this phase of testing, carbon-fiber-reinforced polymer (CFRP) wraps were used for the additional confinement. The axial loading test matrix and the results of load carrying capaci-

Table 1. Axial Compression Test Matrix and Main Results

Specimen name	Test type	Maximum load (kN)
CY-1	Plain concrete cylinder[a]	790
CY-2		893
CY-3		869
HT	Hollow steel tube[b]	492
CFT	Concrete filled steel tube	1,453
CCFT-2L-1	Confined CFT by two layer CFRP[c]	2,233
CCFT-2L-2		2,266
CCFT-2LG-1	Confined CFT by two layer CFRP with gap	2,214
CCFT-2LG-2		2,136
CCFT-4L-1	Confined CFT by four layer CFRP	3,439
CCFT-4L-2		3,438
CCFT-4LG-1	Confined CFT by four layer CFRP with gap	2,737
CCFT-4LG-2		3,201

[a]Average concrete compressive strength, $f'_c = 46.6$ MPa.

[b]Diameter, $D = 152$ mm; thickness, $t = 2.95$ mm; yield strength, $F_y = 356$ MPa; same tube was also provided for CFT and all CCFT specimens.

[c]Nominal thickness per layer, $t_{jl} = 1.4$ mm/layer; rupture strength, $f_{ju} = 897$ MPa; elastic modulus, $E_j = 64.9$ GPa.

ties are shown in Table 1. Three plain concrete cylinders with a diameter of 152 mm were first tested to provide the compressive strength of the concrete used in all the specimens. One hollow steel tube and one conventional CFT specimen were tested to provide the benchmark behavior data. Eight CCFT specimens with CFRP confinement were tested. Testing parameters for the CCFT specimens were the number of layers of CFRP wraps and with or without the gap between the steel tube and the CFRP confinement. The gap was made with 1-mm-thick soft foam tapes affixed on the surface of the steel tube to provide a cushion effect. Such cushion effect was designed to delay the participation of the CFRP wraps for possibly maximizing the deformability while minimizing the unnecessary strength enhancement.

Compression Test Results

As an example, Fig. 4 compares the axial load and strain relationships for the CFT cylinder and the CFRP confined CFT cylinders with or without a gap between the steel tube and the additional CFRP confinement. As demonstrated in Fig. 4, the use of additional confinement in the CCFT cylinders significantly improved the mechanical behavior of the CFT cylinders, with drastically increased load carrying capacity until the rupture of the CFRP wraps. It is also noticed that though a sudden drop of the load carrying capacity followed the rupture of the CFRP jacket, a capacity slightly higher than that of the CFT specimen can be maintained by the CCFT specimens until large axial strains.

The CCFT cylinders without cushion gap, CCFT-2L-1 and CCFT-2L-2, showed a bilinear feature similar to CFRP confined concrete (Xiao and Wu 2000), prior to the rupture of the CFRP wrap. Due to the existence of the cushion gap between the steel tube and the CFRP wrap, specimens CCFT-2LG-1 and CCFT-2LG-2 had an identical behavior as that of the CFT specimen up to an axial strain of about 0.015, where plastic local buckling of the steel tube became apparent. Measurement of the transverse strain of the CCFT-2LG specimens showed that the CFRP jacket confinement was activated after this stage, as shown in Fig. 4(b). As a consequence of the delayed participation of the CFRP, the

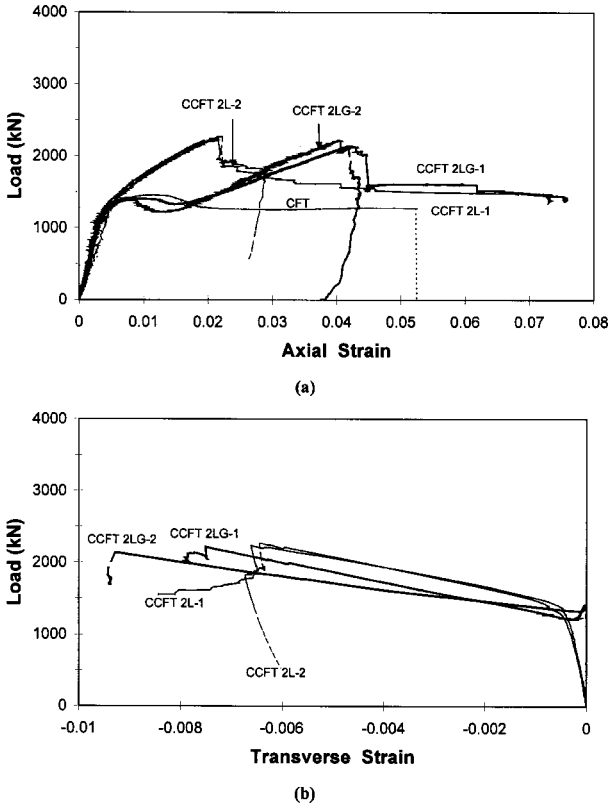

Fig. 4. Axial load–strain relationships for CFT cylinder and CFRP confined CFT cylinders

load carrying capacities of the CCFT-2LG specimens increased again until the rupture of the jacket. Comparing with the CCFT-2L specimens, providing the cushion gap in the CCFT-2LG specimens significantly increased the axial deformability at the CFRP jacket rupture. Similar results were also obtained for specimens with four layers of CFRP confinement.

In the subsequent seismic testing program, a similar cushion gap using foam tapes was also provided to the CCFT model columns with circular sections in order to achieve larger ductility prior to the rupture of the CCFT wraps. Providing such a cushion may also be needed in actual applications due to the fact that CFRP has a smaller thermoexpansion ratio than that of steel.

Seismic Testing Program

Specimen Design

Following the success of the basic axial compression tests, seismic testing validation of the CCFT concept then took place at the Hunan University. Four large-scale model CFT and CCFT columns were designed to simulate typical columns in multistory buildings in seismic regions. The testing matrix is shown in Table 2 and the basic details of the CFT columns are illustrated in Fig. 5. The model column specimens had a circular section with a diameter of 325 mm, and a height of 1,500 mm from the point of lateral loading to the top of the footing. Thickness of the steel tube was 3 mm for two columns and 6 mm for the others.

There was no special confinement for model columns C1-CFT3 for C3-CFT6 for providing benchmark data of seismic behavior of conventional CFT columns. CFRP was used to provide

Table 2. Seismic Loading Test Matrix

Specimen	Section shape	Steel tube thickness (mm)	Steel tube D/t ratio	Steel yield strength F_y (MPa)	Confinement	Concrete strength f'_c (MPa)
C1-CFT3	Circular $D=336$ mm	3.0	112	303	—	39.1
C2-CCFT3			—		CFRP[a]	39.1
C3-CFT6	Circular $D=325$ mm	6.0	54	312	—	28.0
C4-CCFT6			—		CFRP[a]	28.0

[a]Nominal thickness, $t_{j1}=0.22$ mm/layer; rupture strength, $f_{ju}=2,500$ MPa; elastic modulus, $E_j=210$ GPa.

additional confinement to the potential plastic hinge regions of columns C2-CCFT3 and C4-CCFT6. The length of the confined zone was 300 mm, close to the section diameter. The specimens were designed and constructed with a stiff stub footing of 2,000 mm × 700 mm × 420 mm. The stub footings were heavily reinforced to eliminate any premature failure during testing.

Specimen Construction

Material properties for all specimens are summarized in Table 2. The mixture proportions per cubic meter of concrete were 190 kg water; 425 kg Portland cement; 1,211 kg coarse aggregates; and 570 kg fine aggregates. The water-to-cement ratio was 0.45. The maximum dimension of the coarse aggregates was approximately 20 mm. The concrete compressive strength values shown in Table 2 are based on compression tests on 150 mm cubic specimens, however, converted into the cylinder strength, f'_c, by a factor of 0.8. The Chinese standard Q235 grade steel with nominal strength of 235 MPa was used for the steel tube in all the columns. The loading stub and the footing were longitudinally reinforced with Grade III steel with an average yield strength of 345 MPa and transversely reinforced with Grade II steel with an average yield strength of 215 MPa. The tensile strength and the modulus of the unidirectional CFRP sheets used for confining the two circular CCFT columns were 2,500 and 210 GPa, respectively, based on 0.22 mm/layer thick flat coupon tests.

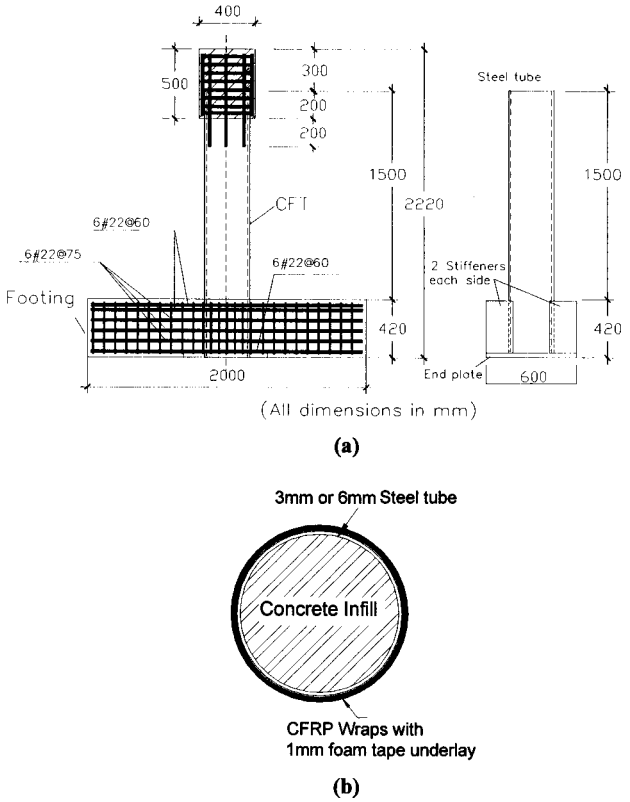

Fig. 5. Specimen details: (a) CFT column portion and (b) confined section details

The 3-mm-thick circular steel tubes were made by a local pressured container manufacturer by rolling steel plate to cylindrical shells and then welding the seam. The 6-mm-thick circular steel tubes were standard pipe products with spiral seam welds. The tubes were first welded to an end plate and stiffeners for the bottom to ensure a strong connection with the stub footing. The tubes were then shipped to the laboratory for preparing the steel caging for the footing and top stub as well as casting concrete. Two specimens were cast together with concrete produced at the laboratory using a forced mixer.

The additional transverse confinement for the two circular CCFT columns was made by four-layer CFRP sheets wrapped around the potential hinge region. Prior to applying the CFRP wrapping, a layer of 1-mm-thick foam tapes were affixed to the surface of the tube to provide a cushion effect based on the basic mechanical testing studies. Fig. 6 shows the process of applying the CFRP wrapping to the potential plastic hinge region of model column C4-CCFT6.

Test Setup

All model columns were tested using the test setup shown in Fig. 7. The test setup, designed by the first and the second writers, can apply lateral loading using a pseudocontrolled hydraulic actuator to a large-scale model column in a condition of vertical cantilever. A constant axial load of 2,000 kN was applied to the column through posttensioning two 50-mm-diameter high-strength steel rods using two 1,500 kN capacity hydraulic hollow jacks. The forces of the rods were transferred to the model column by a cross beam mounted on top of the load stub. In order to eliminate the bending of the high-strength rods, a specially designed pin device was connected to the lower end of each rod.

The axial load applied to the column was measured by a set of strain gauges affixed on the high-strength rods. The imposed lateral displacement was measured by both the displace transducer of the actuator and a separate linear potentiometer. The corresponding lateral force was recorded by the built-in load cell of the actuator. Electrical resistance strain gauges were affixed on the surfaces of the steel tube and the additional confinement CFRP near the column end.

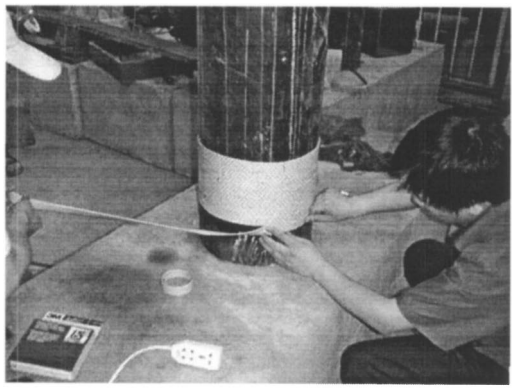

(a)

(b)

Fig. 6. CFRP wrapping: (a) applying foam tape and (b) applying CFRP wrapping

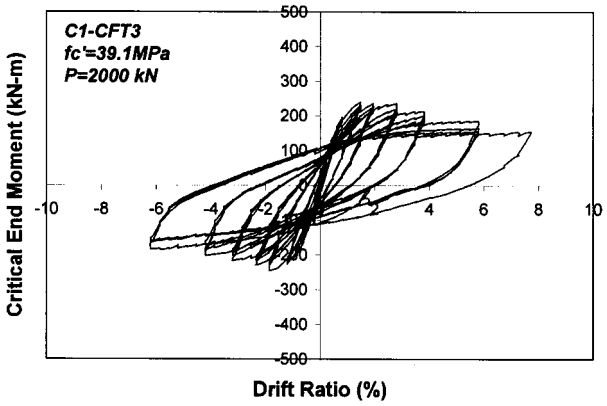

(a)

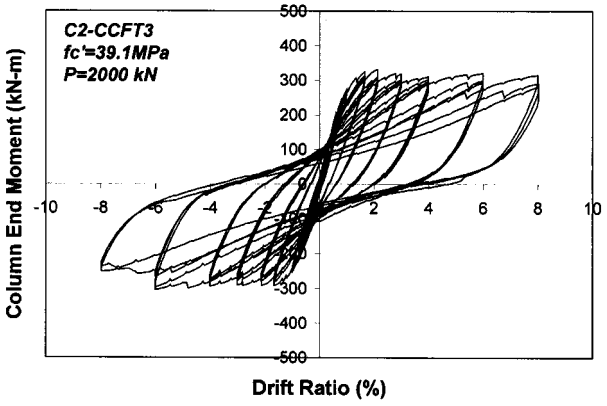

(b)

Fig. 8. Test results of circular specimens with 3-mm-thick steel tube: (a) CFT column and (b) CCFT column with CFRP

Loading Program

During testing, the axial load was maintained constant by the hydraulic system, whereas the lateral force was cycled under a lateral displacement control condition. Three single cycles were initially applied corresponding to an increment of 0.25% peak drift ratio, Δ/L, here Δ=lateral displacement and L=clear length of the model column measured between the application point of the lateral force and the top of the footing. Then, three repetitive loading cycles were applied for each of the peak drift ratios, Δ/L=1, 1.5, 2, 3, 4, 6, 8, and 10%. Such standard loading procedure was attempted until the stage where the model column under testing was judged as unsuitable for further loading.

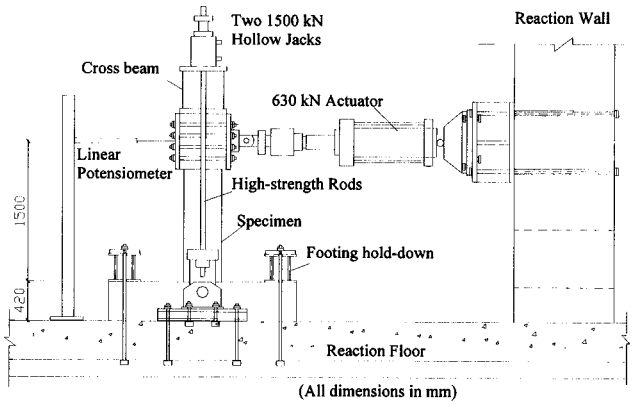

Fig. 7. Test setup

Discussion on Hysteretic Response and Failure Pattern

The hysteretic responses of the column end moment and the drift ratio for all the model columns are shown in Figs. 8 and 9. The calculation of the column end moment included the effects contributed by the axial loading system.

CFT Columns

As shown in Fig. 8(a), circular CFT model column C1-CFT3 with a D/t ratio of 112 had a stable behavior only until cycles corresponding to a peak drift ratio of 2% in the push direction whereas 1.5% in the pull direction. At these stages, the so-called "elephant foot" type local buckling of the steel tube was observed at the position about 20 mm from the bottom end of the column. In the subsequent loading cycles, the local buckling of the steel tube severed, forming several cripples in the column end region with a length approximately equal to the diameter, as shown in Fig. 10(a). During the loading cycles corresponding to a peak drift ratio exceeding 3%, the column sections within the end region expanded drastically indicating the insufficient lateral confinement provided only by the thin steel tube. The moment carrying capacity degraded below 80% of the maximum value at 4% peak drift ratio in the pull loading direction. The loading was continued until the loss of the axial loading capacity during the first cycle at

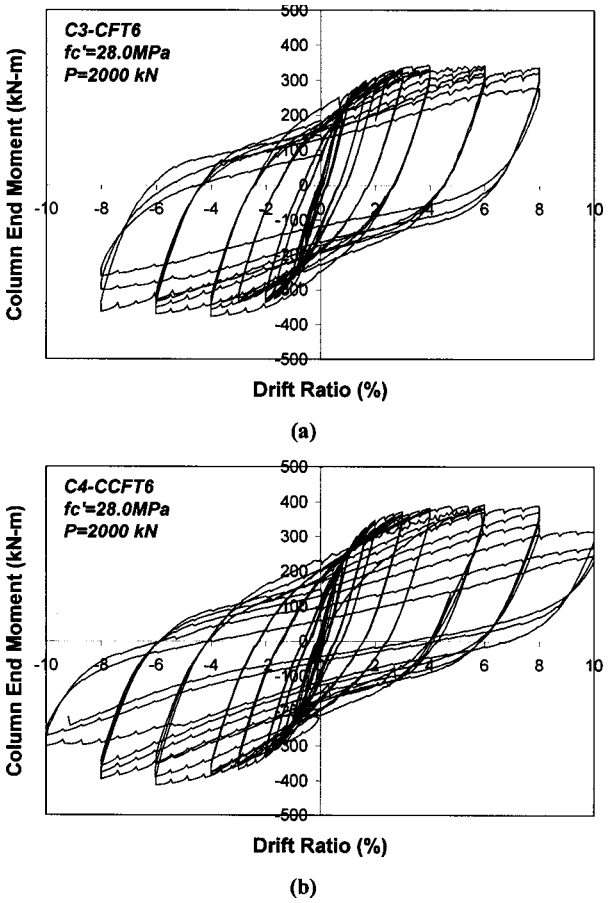

Fig. 9. Test results of circular specimens with 6-mm-thick steel tube: (a) CFT column and (b) CCFT column with CFRP

Fig. 10. Final failure patterns of CFT model columns: (a) CFT column with 3-mm-thick tube or $D/t=112$ and (b) CFT column with 6-mm-thick tube or $D/t=54$.

8%. At the end of the test, the model column shortened for more than 1%, due to the steel tube buckling and crushing of core concrete near column end. The observations were similar to those made by Sakino and Tomii (1981) on relatively smaller scale CFT model columns. Despite significant expansion and crippling, no rupture was observed in the 3-mm-thick steel tube.

As shown in Fig. 9(a), with a thicker tube, the CFT model C3-CFT6 behaved satisfactorily until a drift ratio of 8%. Local buckling and low cycle fatigue caused a rupture of the steel tube along the circular section at a height of about 50 mm, as shown in Fig. 10(b). Powderlike crushed concrete was seen leaking out from the ruptured steel tube. At the end of testing, the specimen also lost about 1% of its original height.

CCFT Columns

Drastically improved behavior can be seen from Fig. 8(b) for CCFT model column C2-CCFT3. The additional CFRP jacket wrapped in the potential plastic hinge region effectively restrained the local buckling of the steel tube and provided better confinement to the section. As the consequence, the CCFT column was able to develop a ductile and stable hysteretic behavior until a peak drift ratio of 8%, where the test was terminated. Rupture of the CFRP jacket near the column end was observed during the cycles corresponding to a drift ratio of 6%. The first rupture was initiated in the compression side of the column at a height of about 30 mm above the footing. The "elephant foot" type local buckling was then formed at the position where the CFRP ruptured. Local buckling was also observed above the CFRP wrapped portion, however, the rest of the confined portion was in good shape, as exhibited in Fig. 11(a). It is apparent that the delaying of local buckling of the steel tube and efficient confinement contributed to the improved seismic behavior of the CCFT column compared with the counterpart CFT specimen.

CCFT model column C4-CCFT6 also demonstrated improved behavior compared with its counterpart CFT model C3-CCFT6. The column was able to satisfactorily endure the loading cycles corresponding to a drift ratio of 8%. The local buckling of the steel tube was delayed until the rupture of the CFRP near the column lower end. After successful behavior during cycles corresponding to a drift ratio of 8%, the specimen was further loaded for three more cycles at a peak drift ratio of 10%. At this final stage, the steel tube ruptured near the column end, as shown in Fig. 11(b).

To demonstrate the improvement of seismic behavior from using CCFT, the envelopes of end moment and drift ratio relationships for all CFT and CCFT specimens are compared in Fig. 12.

Discussion on Local Buckling and Confinement Mechanisms

A simple analytical model is attempted to explain the complicated buckling and confinement mechanisms of the proposed CCFT, and to provide a simple design approach for the additional confinement. As shown in Fig. 13(a), a unit width strip is considered instead of the cylindrical shell. It is assumed that the strip buckles outward, after axial yielding, forming three hinges and the seg-

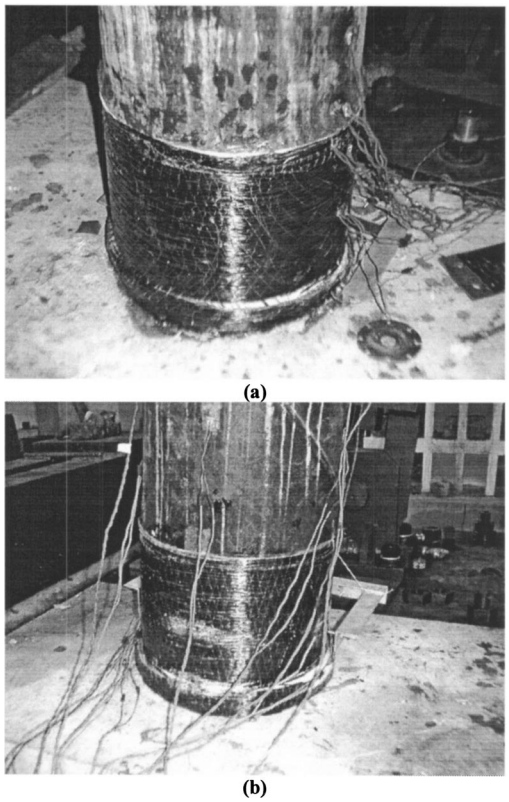

Fig. 11. Condition after testing of CCFT model columns: (a) CCFT column with 3 mm thick tube or $D/t=112$; and (b) CCFT column with 6-mm-thick tube or $D/t=54$.

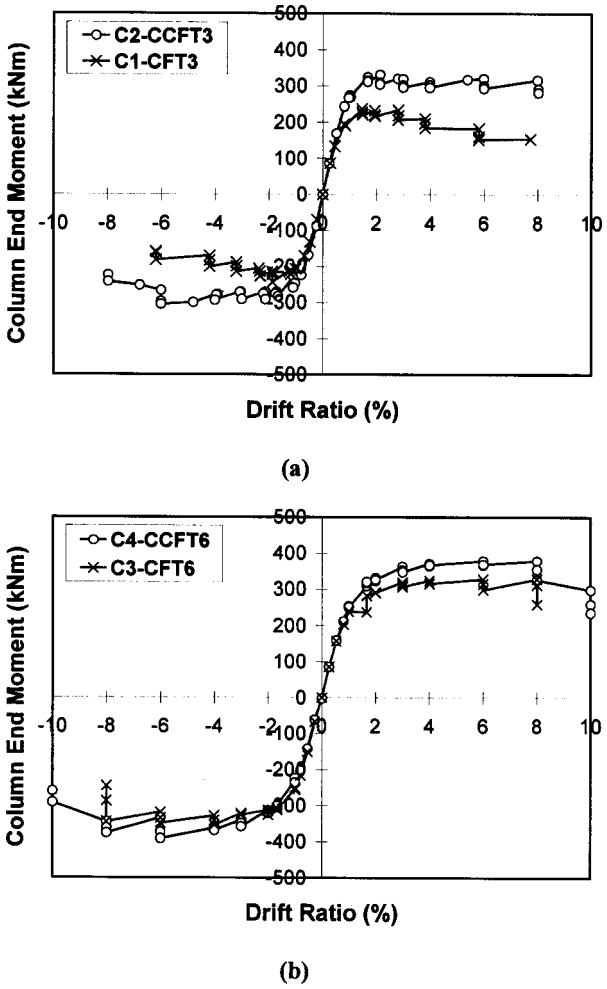

Fig. 12. Comparison of moment–drift ratio envelopes for CFT and CCFT specimens

ments between the hinges are treated as rigid. For a pure elasto-plastic material, to maintain the yield force, $p_y=tf_y$, is impossible. However, for materials with strain hardening, such buckling condition becomes possible. Therefore Shanley's theory (1947) is extended herein to establish the moment resistance for the hinges shown in Fig. 13. For a given radial deformation, δ_r, at the middle hinge, curvature of the concentric hinge can be expressed as $2\delta_r/l^2$, assuming the flexural rotation over a length of $l/2$ is concentrated at the hinge. Thus the moment developed in the hinges of the unit-width strip can be derived as

$$m = \frac{1}{6l^2}[(t+2x)(t-x)^2E_0 + (3t-2x)x^2E_t]\delta_r = m'\delta_r \tag{1}$$

where x=compression zone depth, expressed as

$$x = \frac{1-\sqrt{E_t/E_0}}{1-E_t/E_0}t \tag{2}$$

E_0=elastic modulus; and E_t=tangent modulus of the hardening branch of the stress strain relationship of steel, shown in Fig. 14.

If there is no additional confinement, the equilibrium condition leads to an expression of a buckling length. When additional confinement is provided, equilibrium can be achieved with a larger buckling length. As shown in Fig. 13(b), the confinement stress is linearly distributed along the rigid segment, with the peak at the middle hinge, thus the resultant of the lateral confinement needed for the equilibrium can be derived as follows:

$$F = \frac{3}{2l}(tf_y - 2m')\delta_r \tag{3}$$

Considering the FRP as the perfect elastobrittle material with a rupture limit of ε_{ju}, the limit for the lateral deformation is then

$$\delta_{ju} = g + \varepsilon_{ju} D_j/2 \tag{4}$$

where g=cushion gap provided between the additional confinement and the steel tube; and D_j=diameter of the confinement.

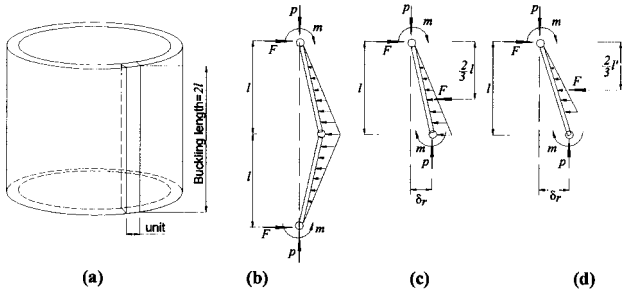

Fig. 13. Analytical model

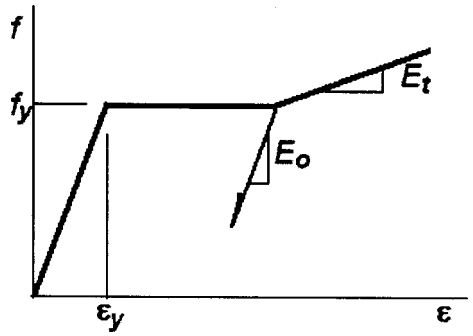

Fig. 14. Stress-strain relationship for steel

If the deformation exceeds the rupture limit of FRP confinement, then only a portion of confinement remains effective as shown in Fig. 13(d). The required confinement force resultant for the equilibrium is then

$$F = \frac{3\delta_r^2}{2l\delta_{ju}}(tf_y - 2m') \tag{5}$$

On the other hand, for a given thickness of the FRP confinement, t_j, the confinement capacity can be expressed as

$$0 \leqslant \delta_r < g, \quad F_j = 0 \tag{6a}$$

$$g < \delta_r \leqslant \delta_{ju}, \quad F_j = \frac{2t_j l}{D_j^2}(\delta_r - g)E_j \leqslant \frac{t_j l f_{ju}}{D_j} \tag{6b}$$

$$\delta_r > \delta_{ju}, \quad F_j = \frac{t_j l f_{ju}}{D_j}\frac{\delta_{ju}}{\delta_r} \tag{6c}$$

where E_j=elastic modulus of FRP.

Fig. 15 shows a numerical example comparing the demand and capacity for the confinement of the CCFT columns with tube thickness of 3 mm and CFRP confinement. In the analysis, the buckling length is assumed to be $2l=0.6D$, based on the suggestions by Sakino and Tomii (1981) for CFT column. As can be seen from the previous equations and Fig. 15, both the demand and the capacity for the confinement are functions of radial deformation. The intersection of the two curves in Fig. 15 represents the failure due to local buckling. The purpose of providing additional confinement is to delay such failure. Based on the analysis, it was found that three layers of CFRP would be sufficient to delay the failure beyond a radial deformation of more than 4 mm, which was approximately assumed based on the observation of test results of the CFT counterpart specimen. In this study, without further analysis, another layer was added to provide confinement for internal concrete.

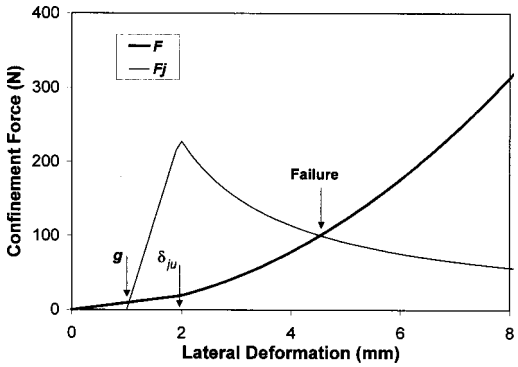

Fig. 15. Numerical comparison of confinement demand and capacity

Conclusions

This paper presented a new CFT column system, named CCFT, in which additional confinement is provided for the potential plastic hinge regions to improve seismic performance. The proposed CCFT columns combine the advantages of a conventional CFT column and the tubed RC column systems. Axial compression tests and seismic loading tests described in this paper successfully validated the writers' concept. In summary, the following conclusions were drawn from this study:

1. As demonstrated from the test results of CFT and CCFT cylindrical stub columns under axial compression, providing additional confinement can significantly increase the axial loading capacity and deformability. CCFT specimens directly wrapped with CFRP exhibited similar bilinear behavior as that of concrete cylinders confined by FRP prior to the rupture of the CFRP.
2. The presence of a cushion gap between the CFRP wraps and the steel tube can postpone the participation of the additional confinement in order to obtain a larger deformability for CCFT prior to the rupture of the CFRP.
3. Achieving satisfactory behavior for CFT model columns subjected to cyclic lateral forces and constant axial load was hindered by the so-called elephant foot type local buckling as well as low-cycle fatigue rupture near the column end and inadequate confinement to the core concrete, particularly for a CFT model column with a thinner steel tube.
4. Seismic behavior of CFT columns can be significantly improved by providing additional confinement to the potential plastic hinge region. As demonstrated by the testing of CCFT model columns with CFRP confinement, the local buckling and subsequent rupture of the steel tube were effectively delayed compared with the counterpart CFT specimens.
5. A simple model based on the modification of Shanley's theory was developed to explain the local buckling and confinement mechanisms. The model can provide certain insight of CCFT design, however, more sophisticated analysis is still underway.

The current phase of the study was focused on the experimental validation to support the writers' idea on the proposed CCFT columns. Research is under way to examine different details for the additional confinement, particularly for noncircular sections.

Acknowledgments

The axial compression tests conducted in this study were made possible at the Structural Laboratory at the University of Southern California (USC), with the donation of materials from the Fyfe Co., California, and SAERTEX, Co., Germany. Main support for the seismic tests conducted at the Structural Laboratory at the Hunan University (HNU) was provided by the Cheung Kong Scholarship awarded to the first writer. Supplemental supports were also provided by the NSF China and the Hunan Provincial Science and Technology Bureau. The writers would like to thank the following gentlemen for their help at various stages during the study: Mr. Hui Wu and Mr. L. Hill of USC; Professor Weijian Yi, Professor Shouping Shang, Professor Yijiang Liu, Professor Yu-

rong Guo, Mr. Bo Shan, Mr. Guowei Zhang, Mr. Weifeng Mao, and Mr. Yuntian Wu of HNU.

Notation

The following symbols are used in this paper:

D = diameter of steel tube;
D_j = diameter of confinement jacket;
E_j = elastic modulus of FRP jacket;
E_0 = elastic modulus of steel;
E_t = tangent modulus of steel;
F = resultant confinement force for a unit strip;
F_j = resultant confinement force provided by FRP;
f'_c = concrete compressive strength;
f_y = steel yield strength;
f_{ju} = circumferential tensile strength of FRP;
g = gap provided between CFT tube and additional confinement;
l = half-buckling length;
m = moment developed in unit-width steel strip;
m' = factor expressed in Eq. (1);
P = applied axial force;
p_y = yield force of unit-width steel strip;
t = thickness of steel tube;
t_j = thickness of required FRP confinement jacket;
δ_r = radial deformation;
δ_{ju} = radial deformation corresponding to ε_{ju}; and
ε_{ju} = circumferential tensile strain limit of FRP, $\varepsilon_{ju}=f_{ju}/E_j$.

References

Aboutaha, R. S., Engelhardt, M. D., Jirsa, J. O., and Kreger, M. E. (1996). "Retrofit of concrete columns with inadequate lap spices by the use of rectangular steel jackets." *The earthquake spectra*, EERI, Oakland, Calif., 693–714.

American Concrete Institute (ACI). (1996). "State-of-the art report on fiber reinforced plastic (FRP) reinforcement for concrete structures." *ACI 440R-96* Committee 440, Detroit.

Chai, Y. H., Priestley, M. J. N., and Seible, F. (1991). "Seismic retrofit of circular bridge columns for enhanced flexural performance." *ACI Struct. J.*, 88(5), 572–484.

Council on Tall Buildings and Urban Habitat. (1992). *Cast-inplace concrete in tall building design and construction—7.3 concrete filled steel tubes*, McGraw-Hill, New York, 202–222.

Moor, W., and Gosain, N. (1985). "Mixed systems: Past practices, recent experience, and future direction." *Proc., Composite and Mixed Construction*, ASCE, New York, 138–149.

Priestley, M. J. N., Seible, F., Xiao, Y., and Verma, R. (1994a). "Steel jacket retrofit of squat RC bridge columns for enhanced shear strength—Part 1—Theoretical considerations and test design." *ACI Struct. J.*, 91(4), 394–405.

Priestley, M. J. N., Seible, F., Xiao, Y., and Verma, R. (1994b). "Steel jacket retrofit of squat RC bridge columns for enhanced shear strength—Part 2—Experimental results." *ACI Struct. J.*, 91(5), 537–551.

Sakino, K., and Tomii, M. (1981). "Hysteretic behavior of concrete filed square steel tubular beam-columns failed in flexure." *Trans. Jpn. Concr. Inst.*, 3, 65–72.

Shanley, F. R. (1947). "Inelastic column theory." *J. Aeronaut. Sci.*, 14/5, 261–267.

Teng, J. G., Chen, J. F., Smith, S. T., and Lam, L. (2000). *RC structures strengthened with FRP composites*, Research Centre for Advanced Technology in Structural Engineering, Department of Civil Engineering, the Hong Kong Polytechnic University.

Tomii, M., Sakino, K., Watanabe, K., and Xiao, Y. (1985a). "Lateral load capacity of reinforced concrete short columns confined by steel tube." *Proc., Int. Speciality Conf. on Concrete Filled Steel Tubular Structures*, Harbin, China, 19–26.

Tomii, M., Sakino, K., and Xiao, Y. (1987). "Ultimate moment of reinforced concrete short columns confined in steel tube." *Proc., Pacific Conf. on Earthquake Engineering, Vol. 2*, New Zealand, 11–22.

Tomii, M., Sakino, K., Xiao, Y., and Watanabe, K. (1985b). "Earthquake resisting hysteretic behavior of reinforced concrete short columns confined by steel tube." *Proc., Int. Speciality Conf. on Concrete Filled Steel Tubular Structures*, Harbin, China, 119–125.

Viest, I. M., Colaco, J. P., Furlong, R. W., Griffis, L. G., Leon, R. T., and Wyllie, L. A., Jr., eds. (1997). *Composite construction design for buildings*, ASCE and McGraw-Hill, Reston, Va. and New York.

Xiao, Y. (2001). "From steel tubed columns to FRP tubed columns." *Proc., ASCE Structural Congress*, Washington, D.C.

Xiao, Y., He, W. H., Mao, X. Y., Choi, K. K., and Zhu, P. S. (2003). "Confinement design of CFT columns for improved seismic performance." *Proc., Int. Workshop on Steel and Concrete Composite Construction (IWSCCC-2003)*, Taipei, R. China, 217–226.

Xiao, Y., and Mahin, S., eds. (2000). "Composite and hybrid structures," *Vols. 1 and 2, Proc., 6th ASCCS Int. Conf.*, Los Angeles, ISBN 0-9679749-0-9.

Xiao, Y., Tomii, M., and Sakino, K. (1986a). "Design method to prevent shear failure of reinforced concrete short circular columns by steel tube confinement (in Japanese)." *Proc., Annual Conf. of Japan Concrete Institute*, 517–520.

Xiao, Y., Tomii, M., and Sakino, K. (1986b). "Experimental study on design method to prevent shear failure of reinforced concrete short circular columns by confining in steel tube." *Trans. Jpn. Concr. Inst.*, 8, 535–542.

Xiao, Y., and Wu, H. (2000). "Compressive behavior of concrete stub columns confined by fiber composite jackets." *J. Mater. Civ. Eng.*, 12(2), 139–146.

Xiao, Y., and Wu, H. (2003). "Retrofit of reinforced concrete columns using partially stiffened steel jackets." *J. Struct. Eng.*, 129(6), 725–732.